RNAseq sheds light on "who is doing what" in the coral *Porites lutea*

Kshitij Tandon[1,2,3*], Juntong Hu[1], Francesco Ricci[4,5], Linda Louise Blackall[1], Mónica Medina[6], Michael Kühl[7], Heroen Verbruggen[1,2,8]

[1]School of BioSciences, The University of Melbourne, Melbourne, VIC 3010, Australia
[2]Melbourne Integrative Genomics, The University of Melbourne, Melbourne, VIC 3010, Australia
[3]Department of Microbiology and Immunology at the Peter Doherty Institute of Infection and Immunity, The University of Melbourne, Melbourne, VIC 3010, Australia
[4]Department of Microbiology, Biomedicine Discovery Institute, Monash University, Clayton, VIC 3800, Australia
[5]Securing Antarctica's Environmental Future, Monash University, Clayton, VIC 3800, Australia
[6]Department of Biology, Pennsylvania State University, University Park, PA 16802, USA
[7]Marine Biological Section, Department of Biology, University of Copenhagen, DK-3000 Helsingør, Denmark
[8]CIBIO, Centro de Investigação em Biodiversidade e Recursos Genéticos, InBIO Laboratório Associado, Campus de Vairão, Universidade do Porto, 4485-661 Vairão, Portugal

*Corresponding author: Kshitij Tandon (k.tandon@unimelb.edu.au)

Abstract

Global decline of coral reefs due to climate change necessitates nature-based protection strategies for these crucial ecosystems. Developing such strategies requires a thorough understanding of the complex roles and interactions occurring within the coral holobiont. Using RNAseq, we investigated the active microbiome of healthy stony coral *Porites lutea*, focusing on the coral tissue, the green endolithic algal layer (*Ostreobiu*m layer), and the deeper coral skeleton. We identified distinct, metabolically active communities within these compartments and highlight substantial metabolic redundancy across carbon, nitrogen, and sulphur pathways. Our study provides first transcriptomic evidence of *Ostreobium's* ability to transfer fixed carbon to other holobiont members and the coral host. Additionally, we highlight critical roles of diverse coral holobiont members in nutrient cycling and maintaining homeostasis through scavenging of reactive oxygen and nitrogen species. This study provides novel molecular-level understanding of the functional roles played by diverse coral holobiont members in their respective compartments and underscores that corals harbour distinct microbiomes with wide-ranging functions.

38 **Introduction**

39 Coral reefs owe their success to the symbiosis between reef-building, stony corals
40 (Scleractinia) (*1–3*) and a large diversity of closely associated bacteria, archaea, viruses, and
41 microeukaryotes, collectively termed the coral holobiont (*3–6*). These symbionts *sensu lato*
42 encompass organisms spanning the full spectrum of host-microbe interactions, from
43 mutualistic partners that enhance coral fitness to opportunistic pathogens, as well as
44 commensals and other microorganisms whose ecological roles may shift along this continuum
45 depending on environmental conditions. While the most well-characterized symbiosis in corals
46 involves photosynthetic, endosymbiotic microalgae in the family Symbiodiniaceae residing in
47 the gastrodermal tissues of the animal host (*7–9*), a compendium of prokaryotes associated
48 with corals has identified 39 bacterial and 2 archaeal phyla (*10*). This diverse microbial
49 assemblage is not only distinct between different compartments within the coral (*11*), but fine-
50 scale mapping of the coral skeleton has revealed a stratified community across its depth (*12–*
51 *14*). In recent years, other microeukaryotes besides Symbiodiniaceae, including endolithic
52 algae of the genus *Ostreobium*, fungi, and apicomplexans have also garnered attention (*15*,
53 *16*).

54

55 The diversity and composition of coral holobiont members have been investigated through
56 metabarcoding of ribosomal marker genes (16S rRNA, 18S rRNA, ITS2) (*17–19*) (*20*, *21*),
57 providing invaluable insights into the diverse and structured symbiont composition *sensu lato*
58 within coral compartments (*12*, *13*, *22*, *23*). Combined culture-based and molecular
59 approaches have expanded our understanding of the functions of coral holobiont members in
60 maintaining coral health and resilience (*24–28*). Symbiodiniaceae, in particular, play a crucial
61 role by supplying corals with photosynthates, meeting a significant portion of their energy
62 demand (*29*). Coral-associated bacteria and archaea have been implicated in a myriad of
63 functions essential for sustaining coral health and resilience, including stress alleviation
64 through scavenging of reactive oxygen and nitrogen species (ROS and RNS), protection
65 against pathogens and nutrient cycling (*24–26*, *28*, *30–32*). Coral skeleton-dwelling endolithic
66 green algae of the genus *Ostreobium,* which form conspicuous green bands beneath the coral
67 tissue, have also been suggested to support corals by providing photosynthates during coral
68 bleaching (*33–35*), but we lack a detailed understanding of the metabolic interaction between
69 the coral animal and *Ostreobium* (*15*).

70

71 Most of our present knowledge on the role of microbiota for coral function and health comes
72 from amplicon and metagenomic sequencing studies, with potential functions inferred using
73 correlative, bioinformatic analyses. Despite these advances and the extensive information now
74 available on the gene-encoded functional potential of microbiome and microeukaryotic

75 members through genomic and metagenomic studies, a significant knowledge gap persists
76 regarding actual microbial metabolic activity and its spatial organisation within the coral
77 holobiont. Genomic data alone cannot predict the actual contributions of specific functions by
78 symbionts *in situ*, as genes encoding these functions may be variably expressed or not
79 expressed at all. RNAseq enables the analysis of the pool of actively expressed genes in an
80 environmental sample, highlighting the ecophysiologically relevant processes occurring at the
81 time of sampling (*36*). Therefore, taking a transcriptomics view can provide insights into which
82 community members perform which functional roles.
83
84 Obtaining a molecular level understanding of the functional roles of holobiont members is
85 crucial especially given the rapid decline of coral reefs worldwide due the adverse effects of
86 climate change (*37*). Addressing this knowledge gap will also be beneficial for developing
87 effective nature-based interventions to protect coral reefs, including improved assisted
88 evolution strategies and development of coral probiotics (*2*, *38*). Both approaches rely on a
89 comprehensive understanding of the roles played by diverse microbial symbionts in
90 maintaining coral health.
91
92 In this study, we sought to answer the fundamental question of 'who is doing what' in a healthy
93 coral holobiont across different compartments. Using RNAseq, we identified the active
94 symbiont community of the coral *Porites lutea*, characterizing their specific activities and
95 locations within the coral, from the tissue to the endolithic algal layer (Ostreobium-layer) and
96 deeper coral skeleton. We focused on key nutrient cycling pathways, including carbon fixation
97 (C), photosynthesis (P), nitrogen (N) and sulfur (S) metabolism, sugar export, and the
98 scavenging of reactive oxygen and nitrogen species (ROS and RNS).
99
100 **Methods:**
101
102 **Coral sampling and colony fragmentation** Fragments from six healthy-looking, *Porites lutea*
103 colonies, spaced at least 15 m apart, were collected at low tide (1-2 m depth) from the research
104 zone of the Heron Island reef flat, southern Great Barrier Reef (23°44′S, 151°91′E), in October
105 2022. Four fragments (from colonies we numbered 1, 3, 4 and 5) were collected during
106 daytime, while two (colonies 6 and 7) were collected five-six hours after sunset. All collected
107 colonies exhibited a visually discernible *Ostreobium-layer* in the coral skeleton . 10-50 mm
108 below the coral tissue layer (Fig. 1A). The fragments were collected using a sterile hammer
109 and chisel and were placed in separate sterile zip-loc polyethylene bags in seawater and flash
110 frozen in liquid nitrogen immediately upon collection. A 5-mm thick slice was cut from the
111 frozen samples, perpendicular to the vertical growth axis, using a diamond saw with a
112 continuous flow of sterile filtered (0.2 µm) seawater. Later, pliers were used to obtain

113 fragments from three distinct layers, i.e., the coral tissue, the green *Ostreobium*-layer, and the
114 tan fraction of the skeleton below the green band (termed the skeleton layer). During this
115 process, the material was kept frozen by repeated immersion in liquid nitrogen. Each layer
116 was kept frozen at -80ºC, transported to the University of Melbourne on dry ice, and processed
117 immediately upon arrival.
118
119 **Total RNA extraction**
120 For RNA extraction, samples of individual layers were ground to a fine powder in liquid nitrogen
121 using pre-cooled mortars and pestles. Approximately 200 mg of powdered tissue samples and
122 between 300-500 mg of powdered *Ostreobium-layer* and skeleton layer were used for RNA
123 extraction with 1 mL of pre-cooled TRIzol reagent (Invitrogen, USA). Total RNA was extracted
124 following the manufacturer's protocol with some modifications (**see supplementary file 1 for**
125 **details**). Quantification of total RNA was conducted using the Qubit RNA HS Assay kit
126 (Thermo Fisher Scientific, USA).
127
128 **RNA sequencing and data-preprocessing**
129 We did not perform any ribosomal RNA depletion due to the dual aim of sequencing mRNA
130 and rRNA from both eukaryotes and prokaryotes simultaneously and profiling the
131 transcriptionally active microbial and microeukaryotic community composition using 16S and
132 18S rRNA abundance (see below). Total RNA libraries were prepared for 36 samples (6
133 colonies x 3 layers x 2 replicates per layer) and sequenced on the Illumina NovaSeq platform
134 by Azenta (Suzhou, China). Sequencing yielded approximately 23 million reads per sample
135 with 2x150 bp reads.
136
137 Raw reads were quality checked and trimmed using FastQC v0.11.9
138 (https://www.bioinformatics.babraham.ac.uk/projects/fastqc) and Trimmomatic v0.39(*39*),
139 respectively. Trimmomatic parameters were as follows: *TruSeq3-PE.fa:2:30:5 HEADCROP:5*
140 *SLIDINGWINDOW:4:20 MINLEN:50*. Quality-filtered reads were first used to identify and filter
141 out rRNA reads using SortMeRNA v4.3.6(*40*) with Silva v138.1 LSU and SSU (*SILVA138.1*
142 *LSU and SSU NR99 database, last accessed Feb 10, 2023*)(*41*). Reads identified as rRNA
143 were taxonomically classified using PhyloFlash v3.4(*42*) (with *almost-everything*), which
144 rapidly reconstructs the SSU rRNAs (NTUs, nearest taxonomic units) and taxonomically
145 annotates them using Silva 138.1 NR99 SSU database. Reads identified as rRNA were
146 removed from the raw-read set, and non-rRNA reads were mapped to the *Porites lutea*
147 genome (accessed from www.reefgenomics.org) using bowtie2 v2.3.4.1(*43*) and samtools
148 1.17(*44*) to identify and remove host-related reads.

149 High-quality, non-rRNA and non-host reads were co-assembled using Trinity v2.15.1(*45*) with
150 parameters *--min_contig_length 250 and --no_salmon*. Taxonomic annotation of assembled
151 transcripts was obtained using the lowest common ancestor approach by performing *blastx*
152 *(46)* searches against the NR database (last accessed April 2023) with diamond
153 v2.1.6.160(*47*), using an *e-value cutoff of 1e-5* and processed through MEGAN6 community
154 edition v6.24.20, using the *megan-map-Feb2022-ue.db* and meganising the *daa* file using
155 *daa2info* (*48*). This process was used to identify and remove any transcripts annotated as
156 Scleractinia and other Eumetazoa. The remaining transcripts were quantified using RSEM
157 (RNA-Seq by Expectation and Maximisation)(*49*), implemented in Trinity through the utility
158 script *align_and_estimate_abundance.pl*. This approach generated both gene and isoform
159 expression profiles. Isoform-level expression data was used for the analysis. Expression
160 values per transcript were averaged across replicates for each layer (tissue, *Ostreobium*-layer
161 and skeleton).
162
163 **Community composition analysis**
164 Taxonomic classification of NTUs assembled from rRNA reads was conducted to profile the
165 abundance of transcriptionally active community members. NTUs classified as "Chloroplast"
166 or "Mitochondria" were removed. Abundance values were converted to relative abundance for
167 compositional analysis using barplots and log-transformed for diversity analysis using PCoA.
168 These analyses were performed using R packages phyloseq v1.42.0(*50*), metagMisc v0.5.0
169 (https://github.com/vmikk/metagMisc) and ggplot2 v34.3 (*51*). We used the quantified and
170 taxonomically annotated transcripts assembled from mRNA reads to profile the community
171 composition encoding for different functional guilds based on the transcriptome data and
172 compared them to rRNA based analysis using the same approach.
173
174 **Functional analysis**
175 To ascertain functional roles, we first filtered transcripts using Trimmed Mean of the M (TMM)
176 values of 0.1 and presence in at least 2 samples to identify truly expressed transcripts. This
177 approach filters out i) any transcripts from potential residual DNA or very low expressed
178 transcripts, ii) transcripts originating from spurious mapping of reads. Transcripts deemed truly
179 expressed were then grouped in a compartment-specific manner to obtain tissue, *Ostreobium*-
180 layer and skeleton-layer specific transcriptome. These compartment specific transcripts were
181 processed through Trinotate v4.0.0(*52*) and Transdecoder v4
182 (https://github.com/TransDecoder/TransDecoder) to identify the longest open reading frames
183 and predict the proteins from transcripts ≥50 amino acids. Predicted proteins were functionally
184 annotated using a combination of EggNOG mapper v2.1.12(*53*) with database eggnogDB

185 v5.0.2(*54*) with *e-value cutoff 1e-5*, ghostkoala (*55*) with database
186 *c_family_euk+genus_prok+viruses* parameters and Interproscan v5.63-95.0(*56*) with *e value*
187 *cutoff 1e-5* to obtain a comprehensive understanding of functional orthologous groups
188 (EggNOG and COG), KEGG pathways, including Kegg Ontology, KOs and protein families
189 (pfam). Metabolic markers for carbon-fixation (C), photosynthesis (P), nitrogen (N) and sulfur
190 (S) metabolism were identified from a previous study (*57*). Additionally, we focussed on genes
191 involved in sugar export and scavenging of ROS and RNS. Expression profiles of transcripts
192 functionally annotated with marker KOs or pfams were plotted using heatmaps using
193 ComplexHeatmap(*58*) in R.
194
195 **Results and Discussion**
196
197 **Corals harbor compartment-specific active symbiont community**
198
199 One of our primary objectives was to profile the transcriptionally active community within the
200 coral holobiont and compare these findings with the community composition obtained from
201 rRNA analysis. To achieve this, we examined the total and active community composition
202 across the coral tissue, the endolithic *Ostreobium-layer*, and the underlying coral skeleton,
203 and compared it with their rRNA based community composition (**Fig 1A)**. For total community
204 composition, we taxonomically analysed 28,717 rRNA NTUs (6,010 from tissue layer, 15,942
205 from *Ostreobium* layer, 26,712 from skeleton layer) belonging to Archaea (2.92% - 840
206 sequences), Eukaryota (12.68% - 3,644 sequences), and Bacteria (84.38% - 24,233
207 sequences) (**Fig 1B**). This observation offers essential insights into the diversity and
208 composition of the coral holobiont. Unlike traditional amplification-based metabarcoding
209 analyses, which are often biased (*59*) and fail to provide accurate quantitative distinctions
210 between prokaryotes and eukaryotes, using rRNAs assembled from total RNA delivers a more
211 precise and comprehensive overview of the community composition. Eukaryotes (Amorphea,
212 SAR, Archaeplastida) were the dominant groups in the coral tissue (**Supplementary Fig S1A**)
213 and the *Ostreobium layer* (**Supplementary Fig S1B**), while the deeper skeleton was
214 dominated by Bacteria (Proteobacteria, Planctomyceota, Desulfobacteria, and Cyanobacteria)
215 (**Supplementary Fig S1C**). Our study shows that bacterial diversity is highest in the skeleton,
216 where the majority of bacterial NTU sequences were assembled, confirming previous reports
217 of greater bacterial richness in the skeleton compared to tissue compartments (*13*, *19*).
218
219 After initially evaluating NTUs based on rRNAs, we extended our analysis to the remaining
220 RNA sequence annotations. To profile active microbial community composition, we used a
221 curated set of 371,193 taxonomically annotated transcripts, selected from a total of 780,431
222 assembled sequences. After excluding 111,367 transcripts belonging to Scleractinia,

223 Chordata, and Eumetazoa, 259,826 (47.56%) transcripts remained. These transcripts
224 represent Eukaryotes (52.48% - 136,366), Bacteria (44.99% - 116,900), Archaea (1.97% -
225 5,131), and viruses (0.54% - 1,429) (**Fig 1B**) and revealed a high relative abundance of
226 alveolates, the eukaryotic group containing Apicomplexa and dinoflagellates, including
227 Symbiodiniaceae in coral tissue (**Supplementary Fig S2A)**. Green algae, Streptophyta and
228 Chlorophyta, dominated the *Ostreobium layer* and deeper skeleton. (**Supplementary Fig S2B**
229 **and C**). The high relative abundance of dinoflagellate (Symbiodiniaceae) expressed
230 transcripts in coral tissue is unsurprising, as they are the most dominant microeukaryotes in
231 the coral tissue, meeting most of the coral's energy demands (*60*). However, we identified
232 dinoflagellate and Apicomplexa transcripts in all compartments. Apicomplexans have been
233 found in healthy coral colonies across the geographic distribution and taxonomic diversity of
234 corals, but their role is yet to be characterized (*16*, *61*). Bacteria and Fungi were present in all
235 compartments, with bacteria as dominant members of the skeletal microbiome
236 (**Supplementary Figure S2C)**. Proteobacteria, Cyanobacteria and Actinobacteria were the
237 dominant bacterial phyla in all coral compartments. Members of the phylum Proteobacteria
238 are some of the most widespread coral microbiome members (*10*, *17*, *62*). Cyanobacteria
239 have also previously been identified as the dominant prokaryote group in the *Ostreobium layer*
240 and deeper skeleton of *P. lutea* from the Red Sea (*63*). Obtaining annotation for less than 50%
241 of the total assembled transcripts highlights the immense diversity of uncharacterised
242 symbionts associated with *P. lutea,* despite it being one of the best investigated coral species
243 with several metagenomic and physiological studies (*24*, *25*, *64*, *65*). These findings align with
244 earlier studies using the metatranscriptomics approach to profile transcriptionally active
245 microbiomes in other ecologically diverse systems, including soil (*66*–*68*), sponge (*69*) and
246 ocean microbiomes (*57*, *70*).

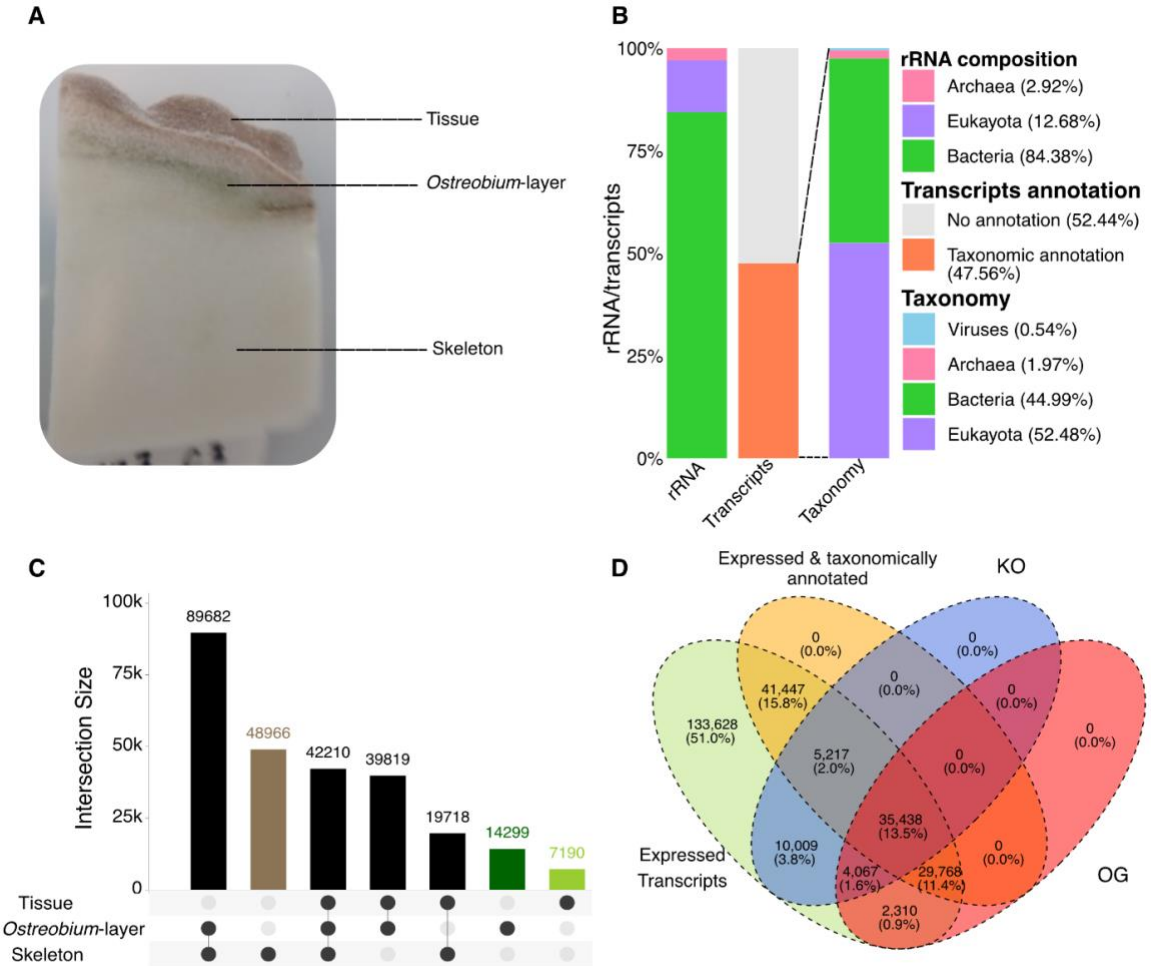

Fig. 1. Taxonomic and functional overview based on rRNA and transcriptome data A) illustration of a coral fragment depicting the three compartments: Tissue, Ostreobium-layer and Skeleton. B) Bar plots showing overall community composition based on rRNA and transcriptome data. C) UpSet plot illustrating shared and unique transcripts across different coral compartments. D) Venn diagram showing counts and percentage of transcripts which are deemed expressed, expressed and taxonomically annotated, annotated at KO and at OG levels.

Functional annotation of transcripts remains a bottleneck

Analysis of active metabolic pathways in a healthy coral holobiont revealed 261,884 truly expressed transcripts through TMM filtering. These transcripts were distributed across the three investigated compartments, with the highest overlap observed between the *Ostreobium layer* and deeper skeleton (89,682 shared transcripts). Additionally, a substantial number of uniquely expressed transcripts were identified in the deeper skeleton-layer (48,966), while the coral tissue exhibited the lowest count of uniquely expressed transcripts (**Fig. 1C**). Recent metabarcoding and metagenomic studies have highlighted the skeleton as the most diverse compartment of corals (*13*, *19*, *63*). In line with these observations, our coral skeleton samples

266 revealed 178,580 uniquely predicted proteins from the expressed transcripts. However, only
267 30.64% (54,731) could be annotated using KO ids and 29.25% (52,252) using OGs (**Fig 1D**).
268 The extraordinary uniqueness of skeletal proteins underscores the added value of sampling
269 genomically underexplored environments, such as the coral skeleton. The low functional
270 annotation observed in our dataset is consistent with a recent study on gene expression
271 changes and community turnover of global oceans, which similarly found less than 25% of the
272 transcripts assigned to KOs (*57*). Annotations based on COG revealed a notable proportion
273 of proteins encoded by transcripts involved in signal transduction, intracellular trafficking,
274 secretion, vesicular transport, post-translational modification, protein turnover, and
275 chaperones (**Supplementary Figure S3)**. While most transcripts remained unannotated, the
276 presence of these functional categories suggests potential microbial involvement in cellular
277 communication and protein homeostasis within the coral holobiont. Although our data do not
278 directly demonstrate nutrient or metabolite exchange, these functional signals are consistent
279 with prior hypotheses that such microbial activities may support coral resilience, particularly in
280 oligotrophic environments. Further targeted studies, including isotopic tracing or compartment-
281 specific transcriptomics, will be needed to directly test these functional roles.
282
283 **Distinct photosymbionts drive carbon fixation in coral compartments**
284 To reveal the functional roles of transcriptionally active holobiont members in healthy *P. lutea*
285 coral, we identified key microbial processes, such as photosynthesis, carbon fixation, sugar
286 export, and nitrogen and sulphur cycling. Our analysis of pathway-specific metabolic markers
287 highlighted the taxonomic affiliations of transcripts and their expression profiles, shedding light
288 on the active contributions of each microbial group to these essential processes. Among the
289 most highly expressed genes were those associated with photosynthetic carbon fixation,
290 including photosystem I (PsaA, 59 transcripts), photosystem II (PsbA, 67 transcripts) and the
291 Calvin–Benson cycle enzyme, RuBisCO subunits (ribulose-1,5-bisphosphate
292 carboxylase/oxygenase, *rbc*L (79) and *rbc*S (18) genes) (**Fig 2**). While rbcL can be expressed
293 by chemotrophs (*71*), our taxonomic annotations did not identify chemotrophic affiliations,
294 suggesting that carbon fixation in this context is predominantly photoautotrophic. These genes
295 were actively transcribed by Symbiodiniaceae, stramenopiles, Bryopsidales (including the
296 endolithic green alga *Ostreobium*), Cyanobacteria, Gammaproteobacteria, and unclassified
297 Viridiplantae and Chlorophyta in different coral compartments. Symbiodiniaceae dominated
298 expression in the tissue, Cyanobacteria were active throughout all compartments, and
299 *Ostreobium* and other Ulvophyceae were the main contributors in the deeper skeleton layers
300 (**Supplementary data file 2**). The co-expression of *rbc*L/*rbc*S with *psb*A and *psa*A supports
301 the role of chlorophototrophy as the dominant carbon fixation strategy in the coral holobiont
302 (*72–74*).

303

304 In the skeleton, we also detected transcripts indicative of alternative carbon fixation pathways.
305 The expression of *cox*L, *cox*M, and *cox*S, affiliated with Cyanobacteria and Proteobacteria,
306 suggests potential activity of carbon monoxide dehydrogenase (CODH), enabling CO
307 oxidation and energy generation through chemosynthesis. Additionally, transcripts for *acs* and
308 *acs*B, encoding the acetyl-CoA synthase complex of the Wood–Ljungdahl pathway, were
309 expressed in the skeleton and affiliated with anaerobic bacteria. This pathway enables fixation
310 of CO_2 and CO into acetyl-CoA, a central metabolite in microbial energy and biosynthetic
311 pathways (*63*, *75*). These transcriptional signals reflect the metabolic versatility of skeleton-
312 associated microbial communities and suggest adaptation to low-oxygen, possibly CO-rich
313 microenvironments (*14*, *76*). Although we did not directly measure substrate availability or
314 fluxes, the coexistence of phototrophic and anaerobic carbon fixation pathways implies that
315 microbial communities play diverse roles in internal carbon cycling. These findings highlight
316 the functional potential of coral-associated microbes to persist in spatially heterogeneous,
317 nutrient-poor reef environments; however, further experimental work is needed to determine
318 the direct impacts of these processes on coral physiology or holobiont productivity.
319

320 Besides *psa*A and *psb*A, we detected expression of several other photosynthetic marker
321 genes across all three coral holobiont compartments. These included, *petC* , which encodes
322 the Rieske iron–sulfur protein of the cytochrome b6f complex that links Photosystem II to
323 Photosystem I, and *petE* ncoding plastocyanin, which facilitates electron transfer between the
324 cytochrome b6f complex and Photosystem I. The expression of these genes supports the
325 widespread presence of oxygenic phototrophs throughout the coral tissue, *Ostreobium* layer,
326 and skeleton. transcripts for cyanobacteria-specific antenna proteins—including *apcA, apcF,*
327 *cpcA, cpeA* and *cpeT*—were most abundant in the Ostreobium layer and deeper skeleton,
328 suggesting a greater prevalence and transcriptional activity of Cyanobacteria in these
329 compartments compared to the tissue (**Fig 2**). This pattern is consistent with taxonomic
330 assignments based on both rRNA (**Supplementary Fig S1**) and transcriptome levels
331 (Supplementary Fig S2) and aligns with previous findings showing an enrichment of
332 cyanobacterial and eukaryotic phototrophs in the skeletal layers of *P. lutea* These antenna
333 and photosynthetic genes, many of which are involved in the Calvin–Benson cycle, collectively
334 accounted for more than 50% of the total carbon fixation gene transcripts in the skeleton. We
335 also observed expression of *pufM*, a marker gene for anoxygenic photosynthesis that encodes
336 a core component of the bacterial photosynthetic reaction centre. Expression of *pufM* was
337 confined to the skeleton, suggesting the presence of obligate anaerobes, such as green sulfur
338 and purple non-sulfur bacteria. This observation is in agreement with hyperspectral pigment

339 imaging, which revealed pigment signatures consistent with anoxygenic phototrophs in the
340 skeletal layers of *P. lutea* (*14*).
341
342 The observed compartment-specific expression patterns of photosynthetic genes reflect
343 microbial adaptations to distinct light regimes within the coral holobiont and provide insight
344 into the metabolic plasticity of associated phototrophs. The elevated expression of
345 cyanobacterial antenna protein genes (*apcA*, *apcF*, *cpcA*, *cpeA*, *cpeT*) in the Ostreobium
346 layer and deeper skeleton suggests that Cyanobacteria inhabiting these low-light regions may
347 utilize alternative chlorophyll pigments, such as chlorophyll *d* and *f*, to absorb far-red light that
348 penetrates coral tissue. This strategy likely enhances photosynthetic efficiency under reduced
349 irradiance and aligns with previous reports of far-red light utilization by endolithic
350 Cyanobacteria and *Ostreobium* (*77–79*).
351
352 Within the same skeletal microhabitat, the green alga Ostreobium appears to employ
353 complementary adaptations, including the use of chlorophyll b and an expanded suite of light-
354 harvesting complex (LHC) proteins in both photosystems (*15*). Genomic features such as
355 Lhca1 gene duplication and the loss of photoprotective genes further reflect specialization to
356 persist under light-limited conditions (80). In contrast, the tissue compartment, characterized
357 by higher light availability, showed dominant transcriptional activity from Symbiodiniaceae and
358 other phototrophs known to rely on chlorophyll *a*and *c*, consistent with adaptation to higher
359 irradiance (81). The distinct expression of photosynthetic genes and pigment-related functions
360 across coral compartments emphasizes the niche differentiation and photoadaptive strategies
361 among coral-associated phototrophs. These spatial patterns of gene expression illustrate the
362 functional diversity of the holobiont and suggest mechanisms by which microbial communities
363 could contribute to energy capture across microhabitats with steep light gradients.
364
365 **Not only Symbiodiniaceae provide fixed carbon to the coral holobiont**
366 To identify members of the coral holobiont involved in the export of photosynthetically fixed
367 carbon compounds (photosynthates), we focused on genes encoding SWEET ("Sugars Will
368 Eventually be Exported Transporter") proteins. SWEETs are bidirectional sugar uniporters that
369 facilitate the diffusion of sugars such as glucose along concentration gradients across
370 biological membranes (*82*, *83* We identified transcripts encoding SWEET proteins, specifically
371 associated with Pfam domains PF04193 and PF03083, across all three major compartments
372 of the coral holobiont (**Fig 2**). Taxonomic annotation of these transcripts revealed that sugar
373 exporters were predominantly eukaryotic, including Symbiodiniaceae, the endolithic
374 alga *Ostreobium*, and unclassified green algae within the Chlorophyta (**Supplementary data**
375 **file 2**). These organisms share a common capacity for oxygenic photosynthesis via the Calvin

376 cycle, in which glyceraldehyde-3-phosphate (G3P), serves as a precursor for sugar
377 biosynthesis, including glucose. Glucose is likely the principal carbohydrate exported via
378 SWEET proteins (*84*), suggesting that these eukaryotic phototrophs contribute substantially
379 to the pool of photosynthates available within the coral holobiont.
380
381 Interestingly, despite previous studies reporting sugar transporters in coral-associated
382 bacteria (*26*), we did not detect transcripts encoding semiSWEET proteins, the prokaryotic
383 homologs of SWEETs. This absence may reflect a biological partitioning of function; wherein
384 eukaryotic symbionts serve as primary carbohydrate exporters. Alternatively, it could be a
385 result of detection limits or the divergence of bacterial sugar transporters from characterized
386 semiSWEETs. Regardless, our findings highlight a potentially central role for eukaryotes in
387 sugar-based metabolic exchange among holobiont members.
388
389 Notably, we identified SWEET gene expression in *Ostreobium*, providing the first genomic and
390 transcriptomic evidence that this skeleton-dwelling alga has the capacity to export sugars.
391 These sugars may diffuse into the coral skeleton, potentially serving as an energy source for
392 both the coral host and other microbial symbionts. This finding provides molecular support for
393 prior radiolabeling studies using 14C and 13C-labeled photoassimilates , which demonstrated
394 that fixed carbon from endolithic algae can be translocated into coral host lipids under both
395 healthy and bleached conditions (*34*, *35*). The ability of *Ostreobium* to contribute sugars under
396 thermal stress, when Symbiodiniaceae populations are diminished, suggests a compensatory
397 role in mitigating coral energy deficits (*85*). This metabolic capacity may be especially
398 important during bleaching events, offering a survival advantage by partially offsetting the loss
399 of primary photosynthate sources.
400
401 In addition to phototrophs, we also detected the expression of SWEET-encoding transcripts
402 in coral-associated fungi. This is the first direct molecular evidence of fungal participation in
403 sugar transport within the coral holobiont. While the functional implications remain to be fully
404 resolved, fungi are increasingly recognized for their roles in shaping coral-associated
405 microbiomes and reef-scale biogeochemical cycling through nutrient processing and chemical
406 interactions (*86*). Their involvement in fixed carbon exchange may reflect metabolic cross-
407 feeding, carbon recycling, or interactions with other holobiont members, broadening our
408 understanding of fungal contributions to holobiont function.
409
410 The identification of multiple eukaryotic lineages capable of translocating sugars underscores
411 the complex and cooperative nature of carbon cycling within the coral holobiont. These sugar-
412 exporting symbionts likely play critical roles in sustaining coral energy homeostasis. However,

this capability may also pose risks: elevated extracellular sugar concentrations could unintentionally fuel the proliferation of opportunistic or pathogenic bacteria, potentially destabilize the microbial community and compromise coral health. Thus, while eukaryotic sugar exporters contribute to coral resilience, their activity may also influence disease susceptibility, highlighting the need for further investigation into the ecological and evolutionary consequences of carbon transfer dynamics in the coral holobiont.

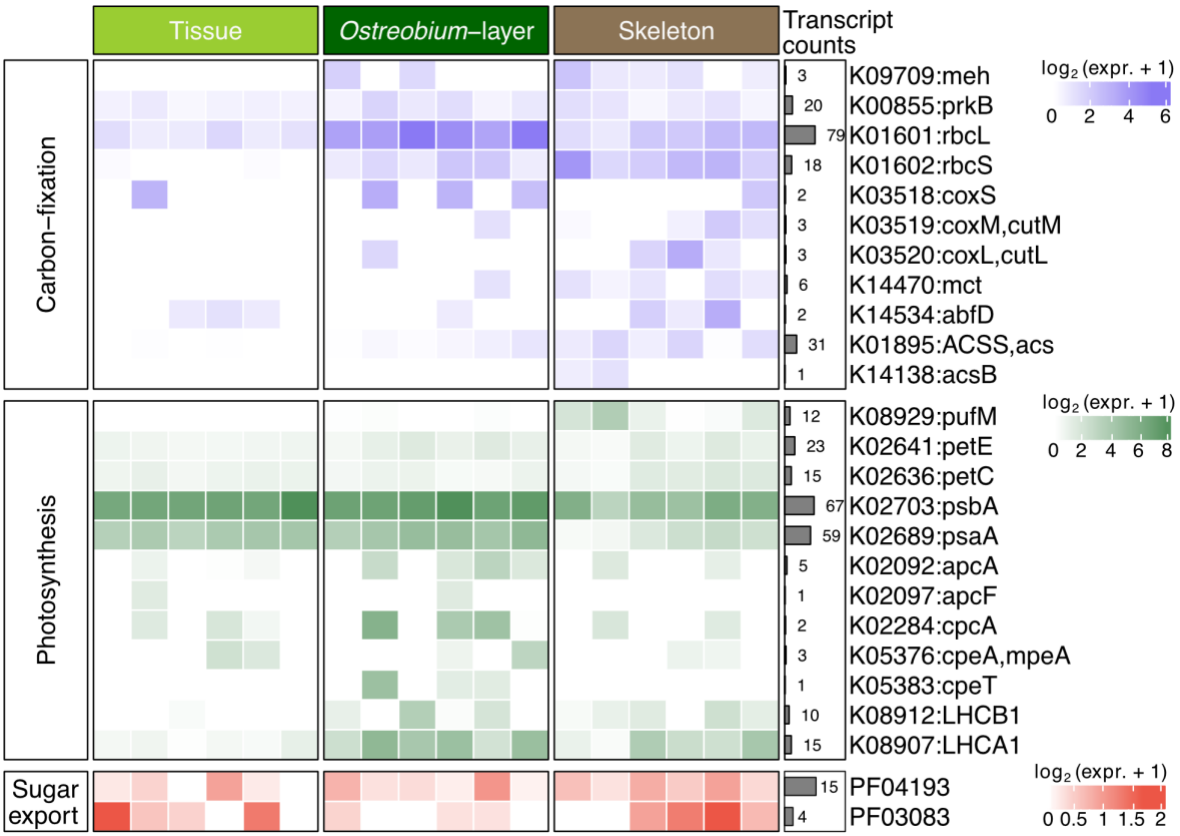

Fig. 2. Carbon Fixation, Photosynthesis and Sugar Export Across Coral Compartments. Heatmap displaying the expression of marker genes for carbon fixation photosynthesis, and SWEET protein-mediated sugar export across various coral compartments. Expression values for both were averaged for the count of transcripts and log2(expression + 1) transformed.

Skeleton dwelling microbes mediate nitrogen metabolism

Our analysis revealed active nitrogen metabolism within the skeleton of *P. lutea*, highlighting the role of skeleton-associated microbes in sustaining nitrogen cycling within the coral holobiont. Expression of canonical nitrogen fixation marker genes nifK, nifD and nifH was detected in both the *Ostreobium* layer and the deeper skeleton, suggesting active nitrogen fixation in these predominantly anoxic microenvironments (**Fig. 3A**). Nitrogen cycling is essential in coral reef ecosystems, where nutrient scarcity demands tight microbial recycling

436 to support coral growth and productivity (*31*). While nitrogen-cycling microbes are widely
437 documented in coral-associated microbiomes (*31*, *87*), our study identified Cyanobacteria as
438 the predominant taxonomically resolved nitrogen fixers in *P. lutea*. This contrasts with earlier
439 reports emphasizing heterotrophic nitrogen-fixing bacteria (*88–90*) and instead aligns with
440 recent genome-resolved metagenomic studies showing low diversity of nitrogen-fixing taxa in
441 this species (*24*, *25*). It is important to note that a substantial proportion of transcripts remain
442 unclassified, and additional nitrogen-fixing taxa may be present but undetected. Nonetheless,
443 the predominance of cyanobacterial transcripts underscores their likely importance in
444 supporting nitrogen-limited growth of Symbiodiniaceae (*9*, *91*), and highlights their key role in
445 the coral holobiont's nitrogen economy.
446
447 We also identified nitrification, the aerobic microbial process converting ammonia to
448 hydroxylamine and subsequently to nitrite and nitrate, to be ubiquitous across all coral
449 compartments (**Fig 3A**). This process is vital for nitrogen turnover and ammonium regulation
450 , reducing toxicity, and maintaining nitrogen turnover within the holobiont, with implications for
451 both coral host and symbiont physiology (*31*). Transcripts encoding nitrification-related genes
452 were primarily assigned to Thaumarchaeota, Gammaproteobacteria, and Chloroflexi,
453 particularly in the deeper skeleton (**Fig 3B and Fig 5**). These taxa likely contribute to ammonia
454 oxidation, although unclassified transcripts and incomplete database coverage suggest that
455 additional nitrifying microbes may be involved.
456
457 In contrast, denitrification was spatially restricted to the *Ostreobium* layer and deeper skeleton
458 compartments, consistent with oxygen-limited conditions in these compartments. We detected
459 expression of key denitrification marker genes (*napA, nirS, norB, and nosZ*) in both eukaryotic
460 phototrophs (Symbiodiniaceae, Ostreobium) and bacterial symbionts, including
461 Rhodospirillales, Chlorobi, Proteobacteria, and Acidobacteria (**Fig. 3A**; **supplementary data**
462 **file 3**). The subsequent steps in denitrification, conversion of nitrite to nitric oxide, nitrous
463 oxide, and nitrogen during denitrification were most commonly attributed to Thaumarchaeota,
464 and Proteobacteria (α- and γ-), and Bacteroidota. Importantly, we also detected fungal
465 (Ascomycota) transcripts encoding NIT-6 gene, involved in dissimilatory nitrate reduction to
466 ammonium (DNRA), providing evidence for fungal contributions to nitrogen recycling within
467 the holobiont.
468
469 The interplay between nitrification, denitrification, and DNRA, particularly within the skeleton,
470 appears crucial for maintaining nitrogen homeostasis. DNRA may dominate under low-oxygen
471 conditions (e.g., at night), recycling nitrate into ammonium when aerobic nitrification is less
472 active. This ensures stable ammonium availability, potentially supporting coral growth. In

473 contrast, coupling of nitrification and denitrification may help regulate nitrogen levels under
474 nutrient-rich conditions, preventing excessive proliferation of Symbiodiniaceae and
475 maintaining a balanced holobiont metabolism.
476
477 Overall, our results expand current understanding of nitrogen cycling in coral holobionts by
478 resolving the microbial taxa actively involved and mapping their compartment-specific
479 activities. The coral skeleton emerges as a metabolically active zone for both aerobic and
480 anaerobic nitrogen transformations, with stratified microbial communities performing
481 complementary functions. These findings underscore the importance of skeleton-associated
482 microbes in holobiont nutrient dynamics and reef ecosystem functioning.
483
484 **Sulphur metabolising microbes are widespread across coral compartments**
485 Sulfur, abundant in seawater primarily as inorganic sulfate, is assimilated by the coral
486 host, Symbiodiniaceae, and various members of the coral microbiome into essential organic
487 compounds, making it a critical element for holobiont growth and function (*92–94*). In this
488 study, we identified expression of transcripts encoding sulfur cycling marker genes across all
489 three coral compartments (Fig. 3B), underscoring the distributed nature of sulfur metabolism
490 within the holobiont. Notably, transcript abundance for most sulfur-related genes was highest
491 in the skeleton, indicating a prominent role for the endolithic microbiome in coral sulfur cycling.
492
493 We detected expression of anaerobic dissimilatory sulfate reduction (DSR) marker genes,
494 aprA and aprB, exclusively in the skeleton compartment. Taxonomic annotation identified
495 these transcripts as originating from canonical sulfate-reducing bacteria (SRB),
496 including Deltaproteobacteria, as well as anoxygenic phototrophic Chlorobi (Fig. 3B).
497 Although Chlorobi carry the aprAB genes, they typically participate in sulfur oxidation rather
498 than sulfate reduction (95, 96), and their presence here suggests diverse sulfur redox
499 processes within the skeleton. This observation supports prior metabarcoding and
500 metagenomic studies, which reported abundant SRBs and assembled their genomes from the
501 skeleton of *P. lutea* and *I. palifera* (24). The co-detection of SRBs and Chlorobi within the
502 same compartment aligns with previous reports of anoxic microniches in coral skeletons (*14*,
503 *24*, *27*, *76*) and suggests the presence of syntrophic interactions, wherein SRB-produced
504 sulfide serves as an electron donor for phototrophic Chlorobi. Such metabolic coupling has
505 been observed in microbial mats, stratified lake waters, and coral skeletons (*27*, *97–99*). The
506 simultaneous expression of aprAB genes by both groups in this study provides molecular
507 evidence for this syntrophy within the coral holobiont.
508
509 We also identified a complex and spatially distributed expression pattern of **assimilatory**

510 sulfate reduction (ASR) genes. Transcripts for cysC, cysI, cysJ, and SUOX were detected
511 across all compartments, whereas cysD expression was restricted to the deeper skeleton (Fig.
512 3B). The gene encoding cysK, which links assimilatory sulfate reduction to L-cysteine
513 biosynthesis, was consistently expressed in all compartments. These findings suggest
514 widespread ASR activity throughout the holobiont, supporting sulfur assimilation and amino
515 acid biosynthesis. Taxonomic analysis of ASR gene transcripts revealed a diverse array
516 of eukaryotic and prokaryotic symbionts. These included microeukaryotes such
517 as Symbiodiniaceae, *Ostreobium*, and other Chlorophyta, as well as bacteria
518 including Cyanobacteria, Thaumarchaeota, and Proteobacteria (Fig. 3B). Notably, all ASR
519 transcripts were exclusively assigned to algae and bacteria, consistent with the known
520 distribution of this pathway among plants, algae, and microbes(*100*).
521
522 Together, these results provide new insights into the compartmentalized and microbially
523 mediated sulfur cycling processes within *P. lutea*. The coral skeleton emerges as a key site
524 for both dissimilatory and assimilatory sulfur transformations, driven by specialized microbial
525 consortia. The detection of potential syntrophic sulfur interactions between SRBs and Chlorobi
526 adds a new layer of complexity to our understanding of the coral skeleton as a metabolically
527 active niche, reinforcing its contribution to holobiont nutrient cycling and resilience.
528

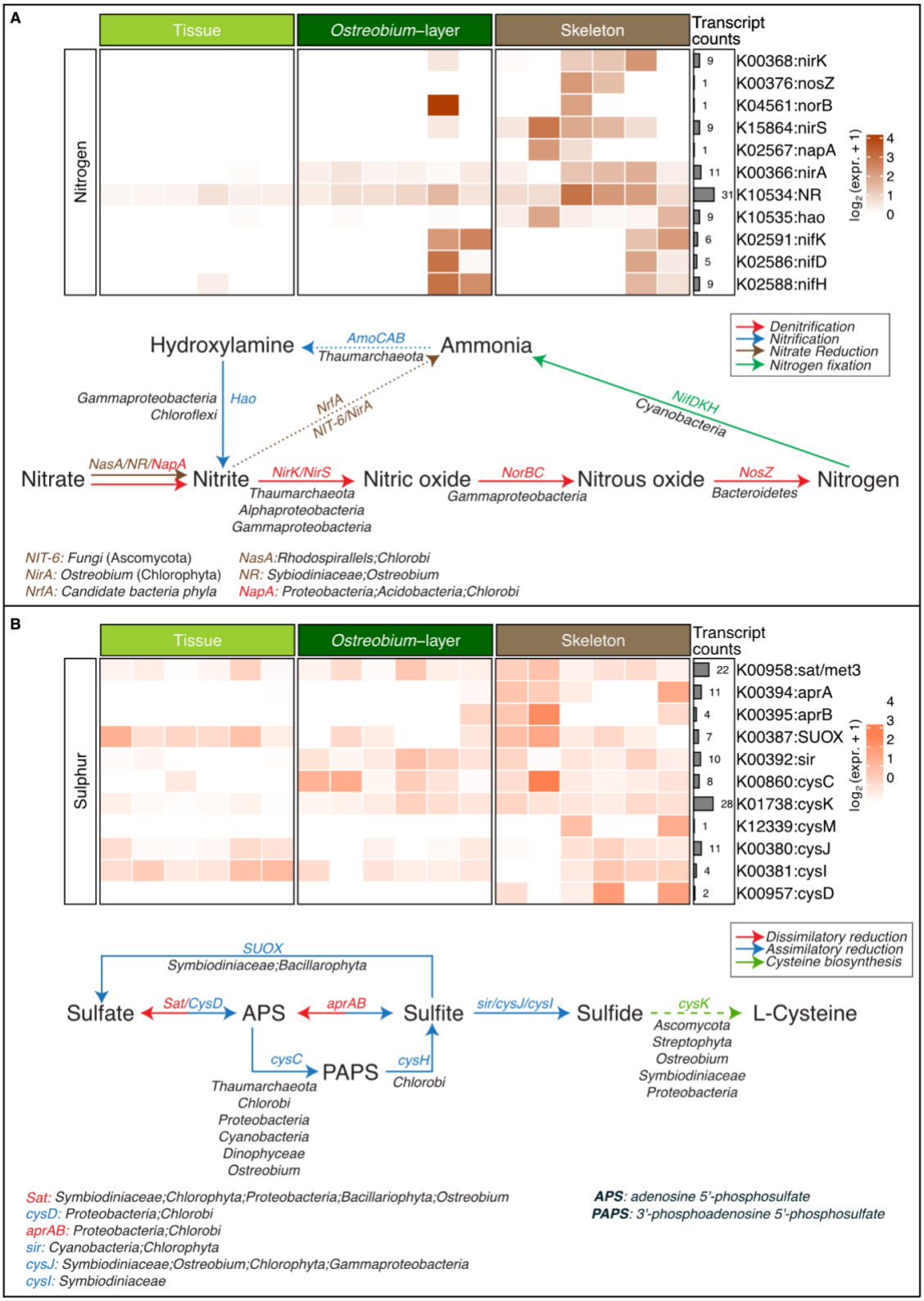

Fig 3. Transcriptome- based expression profiles of Nitrogen and Sulfur metabolism across coral compartments. A) Heatmap showing the expression profiles of marker genes involved in nitrogen metabolism across coral compartments, along with a bar plot indicating the count of transcripts. The nitrogen cycle is illustrated, highlighting subpathways and contributing community members. B) Heatmap showing the expression profiles of marker genes involved in sulphur metabolism across coral compartments, along with a bar plot

536 indicating the count of transcripts. The sulphur metabolism pathway is illustrated, highlighting
537 subpathways and contributing community members. Expression values for both were
538 averaged and log2(expression + 1) transformed.
539
540

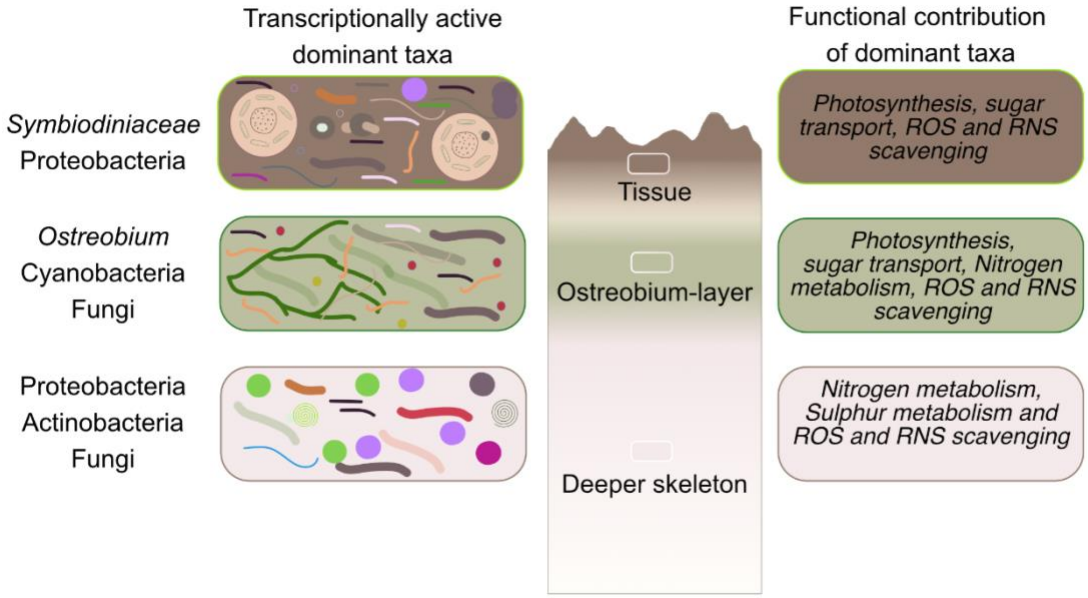

541
542 **Figure 5.** Overview of the transcriptionally dominant taxa and their functional contribution in
543 different compartments of the coral identified in this study.
544
545
546 **Microeukaryotes are the major scavengers of ROS and RNS in *P. lutea***
547 Coral reefs are facing unprecedented threats due to rising sea surface temperatures, resulting
548 in more frequent and prolonged coral bleaching events (*37*). Most theories on the onset of
549 coral bleaching suggest that the overproduction of reactive oxygen species (ROS) and
550 reactive nitrogen species (RNS) is a key trigger, leading to cellular damage and stress under
551 adverse environmental conditions (*101*). Rapid scavenging of ROS and RNS is thus crucial in
552 maintaining homeostasis and protecting the coral holobiont in stressed and healthy corals. We
553 observed widespread expression of seven protein families with functions related to ROS or
554 RNS scavenging across the tissue, *Ostreobium* layer, and deeper skeleton compartments.
555 Specifically, transcripts encoding for genes involved in RNS scavenging, including nitric oxide
556 reductases (PF00175: *hmp*; PF00115 and PF00034: *nor*BC) and peroxynitrite to nitrate
557 reduction (PF10417: *ahp*C) were expressed in all compartments (**Fig 4**). A single transcript
558 encoding nitrous oxide reductase (PF18764: *nos*Z) was identified and expressed exclusively
559 in deeper skeleton samples. This enzyme catalyses the last step of the dissimilatory metabolic
560 pathway of denitrifying bacteria, which were abundant in the deeper skeleton. Similar
561 observations were made for ROS scavenging expression profiles. We identified 48, 43, and

562 41 transcripts encoding the general ROS scavenger Glutaredoxin (PF00462), as well as
563 hydrogen peroxide scavengers Peroxiredoxins (PF00578) and peroxidases (PF00141). These
564 transcripts were expressed in all coral compartments along with transcripts encoding
565 superoxide dismutases (PF00081 and PF02777: SOD Mn and PF00080:SOD cu-zn) (**Fig 4**).
566 The majority of ROS and RNS scavenging transcripts were of micro-eukaryotic origin (76%)**,**
567 including Symbiodiniaceae, *Ostreobium*, Chlorophyta, and Fungi, while others were from
568 archaeal and bacterial sources (24%), encompassing Thaumarchaeota, Proteobacteria
569 (Rhodospirillales, Xanthomonadales), Cyanobacteria, Chlorobi, Chloroflexi and Bacteroidetes
570 (*Candidatus* Amoebophilus) (**Supplementary data file 4**).
571
572 Scavenging reactive oxygen (ROS) and nitrogen species (RNS) is a key function of bacterial
573 candidates for coral probiotics, as emphasised in recent studies identifying potential probiotic
574 bacteria for corals (*2*, *26*, *102–104*). However, the identification of the majority of ROS and
575 RNS scavenging transcripts in micro-eukaryotic inhabitants of the coral holobiont rather than
576 in bacteria, raises the question of which organisms are the main players in scavenging ROS
577 and RNS under thermal stress. This finding suggests that current strategies for designing coral
578 probiotics, which primarily focus on bacterial functions, should be refined through additional
579 molecular and experimental validation to provide functional insights. These insights could
580 guide the assembly of a more comprehensive consortium of beneficial symbionts for corals.
581

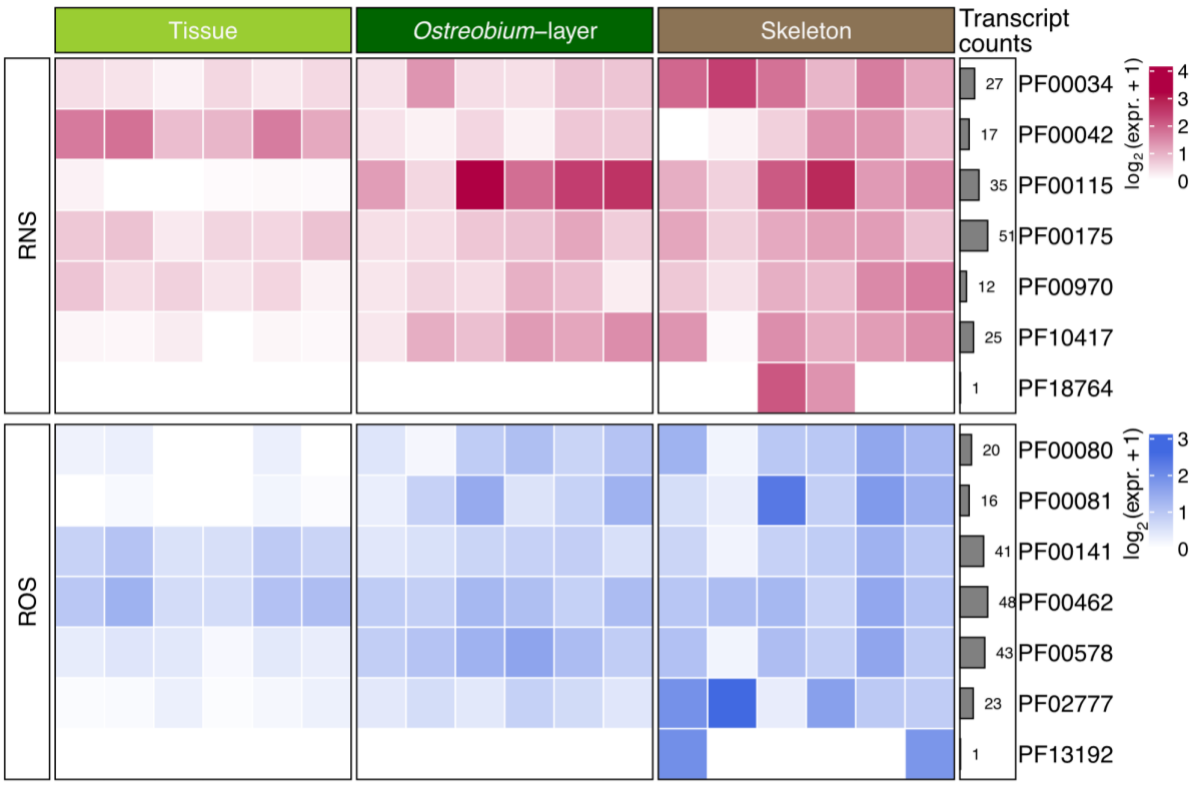

582

583 **Fig. 4. Transcriptome-based expression profiles of Reactive Oxygen Species (ROS) and**
584 **Reactive Nitrogen Species (RNS) marker genes across coral compartments.** Heatmap
585 displaying the expression of different protein families, count of transcripts for each family
586 involved in ROS and RNS scavenging across coral compartments. Expression values for both
587 were averaged and log2(expression + 1) transformed.
588
589
590 **Conclusion**
591 This study provides novel insights into the transcriptionally active communities within the coral
592 holobiont, with a focus on their functional roles across distinct ecological compartments: coral
593 tissue, the endolithic *Ostreobium* layer, and the deeper skeleton layer.
594 Our analysis revealed a nuanced stratification of microbial activity, with microeukaryotes
595 dominating key metabolic processes in the coral tissue and *Ostreobium* layer, while
596 prokaryotes emerge as the primary active symbionts in the deeper skeleton (**Fig 5**). These
597 findings underscore the profound influence of physicochemical gradients—including light
598 penetration, nutrient availability, and carbon distribution—in sculpting both community
599 composition and functional specialization within the holobiont. Functional analysis highlighted
600 the critical contributions of *Symbiodiniaceae, Ostreobium*, and Cyanobacteria to
601 photosynthate production, with *Symbiodiniaceae* predominantly occupying the coral tissue,
602 while *Ostreobium* and Cyanobacteria play pivotal roles in the endolithic *Ostreobium*-layer (**Fig**
603 **5**). These symbionts, evolutionarily adapted to varying light conditions and utilizing distinct
604 photosynthetic pigments, demonstrated unique nutrient cycling capabilities. Notably, in
605 addition to *Symbiodiniaceae*, we identified *Ostreobium* and fungi as the only taxa capable of
606 exporting sugars via SWEET proteins, providing novel insights into nutrient exchange
607 mechanisms within the holobiont. Analysis of nitrogen metabolic pathways revealed
608 Cyanobacteria as the exclusive nitrogen fixers, with other nitrogen and sulphur metabolic
609 processes likely distributed across holobiont members, suggesting a robust functional
610 redundancy that potentially enhances ecosystem resilience (**Fig 5**). Our analysis also
611 identified microeukaryotes as the primary scavengers of ROS and RNS across all
612 compartments, playing a crucial role in maintaining holobiont health, particularly under thermal
613 stress conditions (**Fig 5**). These findings offer a comprehensive view of the metabolic activities
614 within the coral microbiome, elucidating the intricate functional roles of its diverse members.
615 While this research significantly advances our understanding of coral holobiont functions, it
616 simultaneously highlights the complexity of these systems and the necessity for more targeted
617 research focussed on the microenvironmental niches of the coral holobiont. Future
618 investigations should employ advanced sampling techniques and high-resolution analytical
619 methods to more precisely map the functional dynamics between coral hosts, their symbionts,
620 and the surrounding microenvironment (*11*, *105*, *106*). Ultimately, the insights gained from this

621 study are invaluable for advancing coral reef conservation efforts. By identifying functionally
622 relevant symbiotic members, we can better inform the design of coral probiotics and other
623 strategies aimed at enhancing coral resilience in the face of climate change and other
624 environmental stressors.
625
626 **Data and code availability**
627 Raw reads generated in this study have been submitted to NCBI SRA under the Bioproject
628 PRJNA1207708. All codes and files required to regenerate the figures have been made
629 available via github.
630
631 **Acknowledgement**
632 Authors would like to acknowledge staff at the Heron Island Research Station for their
633 assistance during sample collection. All coral samples were collected under Permit
634 G22/47504.1 issued to KT and FR by Great Barrier Reef Marine Park Authority, Australia.
635 Authors would also like to acknowledge reviewers of the manuscript for their suggestions.
636
637 **Funding**
638 This work was funded through the Australian Research Council grant DP200101613 (to H.V.,
639 L.L.B., M.M., and M.K.), the Faculty of Science (University of Melbourne, to H.V.). K.T.
640 acknowledges support from the University of Melbourne Early Career Research Grant. M.K.
641 acknowledges support from the Gordon and Betty Moore Foundation through grant no.
642 GBMF9206 (https://doi.org/10.37807/GBMF9206). M.M. acknowledges support from NOAA
643 CRCP: National Oceanic and Atmospheric Administration Coral Reef Conservation Program
644 NA19NOS4820132. H.V. is supported by the Fundação para a Ciência e a Tecnologia
645 (CEECIND:2023.06155). Computational analysis of this work was supported by the University
646 of Melbourne's Research Computing Services and the Petascale Campus Initiative.
647
648 **References**

649 1. C. Jaspers, S. Fraune, A. E. Arnold, D. J. Miller, T. C. G. Bosch, C. R. Voolstra,
650 Consortium of Australian Academy of Science Boden Research Conference
651 Participants, Resolving structure and function of metaorganisms through a holistic
652 framework combining reductionist and integrative approaches. *Zoology* **133**, 81–87
653 (2019).

654 2. R. S. Peixoto, M. Sweet, H. D. M. Villela, P. Cardoso, T. Thomas, C. R. Voolstra, L. Høj,
655 D. G. Bourne, Coral Probiotics: Premise, Promise, Prospects. *Annu Rev Anim Biosci* **9**,
656 265–288 (2021).

657 3. M. J. H. van Oppen, L. L. Blackall, Coral microbiome dynamics, functions and design in
658 a changing world. *Nat. Rev. Microbiol.* **17**, 557–567 (2019).

659 4. E. Rosenberg, O. Koren, L. Reshef, R. Efrony, I. Zilber-Rosenberg, The role of
660 microorganisms in coral health, disease and evolution. *Nat. Rev. Microbiol.* **5**, 355–362
661 (2007).

662 5. F. Rohwer, V. Seguritan, F. Azam, N. Knowlton, Diversity and distribution of coral-
663 associated bacteria. *Mar. Ecol. Prog. Ser.* **243**, 1–10 (2002).

664 6. R. V. Thurber, J. P. Payet, A. R. Thurber, A. M. S. Correa, Virus-host interactions and
665 their roles in coral reef health and disease. *Nat. Rev. Microbiol.* **15**, 205–216 (2017).

666 7. T. C. LaJeunesse, J. E. Parkinson, P. W. Gabrielson, H. J. Jeong, J. D. Reimer, C. R.
667 Voolstra, S. R. Santos, Systematic Revision of Symbiodiniaceae Highlights the Antiquity
668 and Diversity of Coral Endosymbionts. *Curr. Biol.* **28**, 2570–2580.e6 (2018).

669 8. L. Muscatine, The role of symbiotic algae in carbon and energy flux in reef corals.
670 *Ecosystems of the world* **25**, 75–87 (1990).

671 9. L. A. Morris, C. R. Voolstra, K. M. Quigley, D. G. Bourne, L. K. Bay, Nutrient Availability
672 and Metabolism Affect the Stability of Coral-Symbiodiniaceae Symbioses. *Trends*
673 *Microbiol.* **27**, 678–689 (2019).

674 10. M. J. Huggett, A. Apprill, Coral microbiome database: Integration of sequences reveals
675 high diversity and relatedness of coral-associated microbes. *Environ. Microbiol. Rep.*
676 **11**, 372–385 (2019).

677 11. E. Bollati, D. J. Hughes, D. J. Suggett, J.-B. Raina, M. Kühl, Microscale sampling of the
678 coral gastrovascular cavity reveals a gut-like microbial community. *anim microbiome* **6**
679 (2024).

680 12. M. J. Sweet, A. Croquer, J. C. Bythell, Bacterial assemblages differ between
681 compartments within the coral holobiont. *Coral Reefs* **30**, 39–52 (2011).

682 13. V. R. Marcelino, M. J. van Oppen, H. Verbruggen, Highly structured prokaryote
683 communities exist within the skeleton of coral colonies. *ISME J.* **12**, 300–303 (2018).

684 14. F. Ricci, K. Tandon, M. Moßhammer, E. H.-J. Cho, L. L. Blackall, M. Kühl, H.
685 Verbruggen, Fine-scale mapping of physicochemical and microbial landscapes of the
686 coral skeleton. *Environ. Microbiol.* **25**, 1505–1521 (2023).

687 15. K. Tandon, M. M. Pasella, C. Iha, F. Ricci, J. Hu, C. J. O'Kelly, M. Medina, M. Kühl, H.
688 Verbruggen, Every refuge has its price: Ostreobium as a model for understanding how
689 algae can live in rock and stay in business. *Semin. Cell Dev. Biol.* **134**, 27–36 (2023).

690 16. A. M. Bonacolta, B. A. Weiler, T. Porta-Fitó, M. Sweet, P. Keeling, J. del Campo,
691 Beyond the Symbiodiniaceae: diversity and role of microeukaryotic coral symbionts.
692 *Coral Reefs* **42**, 567–577 (2023).

693 17. M. McCauley, T. L. Goulet, C. R. Jackson, S. Loesgen, Systematic review of cnidarian
694 microbiomes reveals insights into the structure, specificity, and fidelity of marine
695 associations. *Nat. Commun.* **14**, 4899 (2023).

696 18. R. Rowan, D. A. Powers, Ribosomal RNA sequences and the diversity of symbiotic
697 dinoflagellates (zooxanthellae). *Proc. Natl. Acad. Sci. U. S. A.* **89**, 3639–3643 (1992).

698 19. F. J. Pollock, R. McMinds, S. Smith, D. G. Bourne, B. L. Willis, M. Medina, R. V.
699 Thurber, J. R. Zaneveld, Coral-associated bacteria demonstrate phylosymbiosis and
700 cophylogeny. *Nat. Commun.* **9**, 4921 (2018).

20. L. Fujise, D. J. Suggett, M. Stat, T. Kahlke, M. Bunce, S. G. Gardner, S. Goyen, S. Woodcock, P. J. Ralph, J. R. Seymour, N. Siboni, M. R. Nitschke, Unlocking the phylogenetic diversity, primary habitats, and abundances of free-living Symbiodiniaceae on a coral reef. *Mol. Ecol.* **30**, 343–360 (2021).

21. L. K. Lee, C. P. Leaw, L. C. Lee, Z. F. Lim, K. S. Hii, A. A. Chan, H. Gu, P. T. Lim, Molecular diversity and assemblages of coral symbionts (Symbiodiniaceae) in diverse scleractinian coral species. *Mar. Environ. Res.* **179**, 105706 (2022).

22. V. R. Marcelino, K. M. Morrow, M. J. H. van Oppen, D. G. Bourne, H. Verbruggen, Diversity and stability of coral endolithic microbial communities at a naturally high pCO2 reef. *Mol. Ecol.* **26**, 5344–5357 (2017).

23. F. Ricci, A. Fordyce, W. Leggat, L. L. Blackall, T. Ainsworth, H. Verbruggen, Multiple techniques point to oxygenic phototrophs dominating the Isopora palifera skeletal microbiome. *Coral Reefs* **40**, 275–282 (2021).

24. K. Tandon, F. Ricci, J. Costa, M. Medina, M. Kühl, L. L. Blackall, H. Verbruggen, Genomic view of the diversity and functional role of archaea and bacteria in the skeleton of the reef-building corals Porites lutea and Isopora palifera. *Gigascience* **12** (2022).

25. S. J. Robbins, C. M. Singleton, C. X. Chan, L. F. Messer, A. U. Geers, H. Ying, A. Baker, S. C. Bell, K. M. Morrow, M. A. Ragan, D. J. Miller, S. Forêt, ReFuGe2020 Consortium, C. R. Voolstra, G. W. Tyson, D. G. Bourne, A genomic view of the reef-building coral Porites lutea and its microbial symbionts. *Nat Microbiol* **4**, 2090–2100 (2019).

26. T. Doering, K. Tandon, S. H. Topa, S. J. Pidot, L. L. Blackall, M. J. H. van Oppen, Genomic exploration of coral-associated bacteria: identifying probiotic candidates to increase coral bleaching resilience in Galaxea fascicularis. *Microbiome* **11**, 185 (2023).

27. S.-H. Yang, K. Tandon, C.-Y. Lu, N. Wada, C.-J. Shih, S. S.-Y. Hsiao, W.-N. Jane, T.-C. Lee, C.-M. Yang, C.-T. Liu, V. Denis, Y.-T. Wu, L.-T. Wang, L. Huang, D.-C. Lee, Y.-W. Wu, H. Yamashiro, S.-L. Tang, Metagenomic, phylogenetic, and functional characterization of predominant endolithic green sulfur bacteria in the coral Isopora palifera. *Microbiome* **7**, 3 (2019).

28. M. Sweet, H. Villela, T. Keller-Costa, R. Costa, S. Romano, D. G. Bourne, A. Cárdenas, M. J. Huggett, A. H. Kerwin, F. Kuek, M. Medina, J. L. Meyer, M. Müller, F. J. Pollock, M. S. Rappé, M. Sere, K. H. Sharp, C. R. Voolstra, N. Zaccardi, M. Ziegler, R. Peixoto, Insights into the Cultured Bacterial Fraction of Corals. *mSystems* **6**, e0124920 (2021).

29. P. G. Falkowski, Z. Dubinsky, L. Muscatine, J. W. Porter, Light and the Bioenergetics of a Symbiotic Coral. *Bioscience* **34**, 705–709 (1984).

30. K. Tandon, C.-Y. Lu, P.-W. Chiang, N. Wada, S.-H. Yang, Y.-F. Chan, P.-Y. Chen, H.-Y. Chang, Y.-J. Chiou, M.-S. Chou, W.-M. Chen, S.-L. Tang, Comparative genomics: Dominant coral-bacterium Endozoicomonas acroporae metabolizes dimethylsulfoniopropionate (DMSP). *ISME J.* **14**, 1290–1303 (2020).

31. N. Rädecker, C. Pogoreutz, C. R. Voolstra, J. Wiedenmann, C. Wild, Nitrogen cycling in corals: the key to understanding holobiont functioning? *Trends Microbiol.* **23**, 490–497 (2015).

32. M. J. Neave, C. T. Michell, A. Apprill, C. R. Voolstra, Endozoicomonas genomes reveal functional adaptation and plasticity in bacterial strains symbiotically associated with

745 diverse marine hosts. *Sci. Rep.* **7**, 40579 (2017).

746 33. D. Schlichter, H. Kampmann, S. Conrady, Trophic potential and photoecology of
747 endolithic algae living within coral skeletons. *Mar. Ecol.* **18**, 299–317 (1997).

748 34. M. Fine, Y. Loya, Endolithic algae: an alternative source of photoassimilates during
749 coral bleaching. *Proceedings of the Royal Society of London. Series B: Biological*
750 *Sciences* **269**, 1205–1210 (2002).

751 35. L. Sangsawang, B. E. Casareto, H. Ohba, H. M. Vu, A. Meekaew, T. Suzuki, T. Yeemin,
752 Y. Suzuki, 13C and 15N assimilation and organic matter translocation by the endolithic
753 community in the massive coral Porites lutea. *R Soc Open Sci* **4**, 171201 (2017).

754 36. E. A. Ottesen, C. R. Young, S. M. Gifford, J. M. Eppley, R. Marin 3rd, S. C. Schuster, C.
755 A. Scholin, E. F. DeLong, Ocean microbes. Multispecies diel transcriptional oscillations
756 in open ocean heterotrophic bacterial assemblages. *Science* **345**, 207–212 (2014).

757 37. T. P. Hughes, J. T. Kerry, S. R. Connolly, J. G. Álvarez-Romero, C. M. Eakin, S. F.
758 Heron, M. A. Gonzalez, J. Moneghetti, Emergent properties in the responses of tropical
759 corals to recurrent climate extremes. *Curr. Biol.* **31**, 5393–5399.e3 (2021).

760 38. M. J. H. van Oppen, J. K. Oliver, H. M. Putnam, R. D. Gates, Building coral reef
761 resilience through assisted evolution. *Proc. Natl. Acad. Sci. U. S. A.* **112**, 2307–2313
762 (2015).

763 39. A. M. Bolger, M. Lohse, B. Usadel, Trimmomatic: a flexible trimmer for Illumina
764 sequence data. *Bioinformatics* **30**, 2114–2120 (2014).

765 40. E. Kopylova, L. Noé, H. Touzet, SortMeRNA: fast and accurate filtering of ribosomal
766 RNAs in metatranscriptomic data. *Bioinformatics* **28**, 3211–3217 (2012).

767 41. P. Yilmaz, L. W. Parfrey, P. Yarza, J. Gerken, E. Pruesse, C. Quast, T. Schweer, J.
768 Peplies, W. Ludwig, F. O. Glöckner, The SILVA and “All-species Living Tree Project
769 (LTP)” taxonomic frameworks. *Nucleic Acids Res.* **42**, D643–D648 (2013).

770 42. H. R. Gruber-Vodicka, B. K. B. Seah, E. Pruesse, phyloFlash: Rapid Small-Subunit
771 rRNA Profiling and Targeted Assembly from Metagenomes. *mSystems* **5** (2020).

772 43. B. Langmead, S. L. Salzberg, Fast gapped-read alignment with Bowtie 2. *Nat. Methods*
773 **9**, 357–359 (2012).

774 44. H. Li, B. Handsaker, A. Wysoker, T. Fennell, J. Ruan, N. Homer, G. Marth, G. Abecasis,
775 R. Durbin, 1000 Genome Project Data Processing Subgroup, The Sequence
776 Alignment/Map format and SAMtools. *Bioinformatics* **25**, 2078–2079 (2009).

777 45. M. G. Grabherr, B. J. Haas, M. Yassour, J. Z. Levin, D. A. Thompson, I. Amit, X.
778 Adiconis, L. Fan, R. Raychowdhury, Q. Zeng, Z. Chen, E. Mauceli, N. Hacohen, A.
779 Gnirke, N. Rhind, F. di Palma, B. W. Birren, C. Nusbaum, K. Lindblad-Toh, N. Friedman,
780 A. Regev, Full-length transcriptome assembly from RNA-Seq data without a reference
781 genome. *Nat. Biotechnol.* **29**, 644–652 (2011).

782 46. S. F. Altschul, W. Gish, W. Miller, E. W. Myers, D. J. Lipman, Basic local alignment
783 search tool. *J. Mol. Biol.* **215**, 403–410 (1990).

784 47. B. Buchfink, K. Reuter, H.-G. Drost, Sensitive protein alignments at tree-of-life scale
785 using DIAMOND. *Nat. Methods* **18**, 366–368 (2021).

786 48. D. H. Huson, S. Beier, I. Flade, A. Górska, M. El-Hadidi, S. Mitra, H.-J. Ruscheweyh, R.
787 Tappu, MEGAN Community Edition - Interactive Exploration and Analysis of Large-
788 Scale Microbiome Sequencing Data. *PLoS Comput. Biol.* **12**, e1004957 (2016).

789 49. B. Li, C. N. Dewey, RSEM: accurate transcript quantification from RNA-Seq data with or
790 without a reference genome. *BMC Bioinformatics* **12**, 323 (2011).

791 50. P. J. McMurdie, S. Holmes, phyloseq: an R package for reproducible interactive
792 analysis and graphics of microbiome census data. *PLoS One* **8**, e61217 (2013).

793 51. H. Wickham, ggplot2. *Wiley Interdiscip. Rev. Comput. Stat.* **3**, 180–185 (2011).

794 52. D. M. Bryant, K. Johnson, T. DiTommaso, T. Tickle, M. B. Couger, D. Payzin-Dogru, T.
795 J. Lee, N. D. Leigh, T.-H. Kuo, F. G. Davis, J. Bateman, S. Bryant, A. R. Guzikowski, S.
796 L. Tsai, S. Coyne, W. W. Ye, R. M. Freeman Jr, L. Peshkin, C. J. Tabin, A. Regev, B. J.
797 Haas, J. L. Whited, A Tissue-Mapped Axolotl De Novo Transcriptome Enables
798 Identification of Limb Regeneration Factors. *Cell Rep.* **18**, 762–776 (2017).

799 53. C. P. Cantalapiedra, A. Hernández-Plaza, I. Letunic, P. Bork, J. Huerta-Cepas,
800 eggNOG-mapper v2: Functional Annotation, Orthology Assignments, and Domain
801 Prediction at the Metagenomic Scale. *Mol. Biol. Evol.* **38**, 5825–5829 (2021).

802 54. J. Huerta-Cepas, D. Szklarczyk, D. Heller, A. Hernández-Plaza, S. K. Forslund, H.
803 Cook, D. R. Mende, I. Letunic, T. Rattei, L. J. Jensen, C. von Mering, P. Bork, eggNOG
804 5.0: a hierarchical, functionally and phylogenetically annotated orthology resource
805 based on 5090 organisms and 2502 viruses. *Nucleic Acids Res.* **47**, D309–D314 (2019).

806 55. M. Kanehisa, Y. Sato, K. Morishima, BlastKOALA and GhostKOALA: KEGG Tools for
807 Functional Characterization of Genome and Metagenome Sequences. *J. Mol. Biol.* **428**,
808 726–731 (2016).

809 56. P. Jones, D. Binns, H.-Y. Chang, M. Fraser, W. Li, C. McAnulla, H. McWilliam, J.
810 Maslen, A. Mitchell, G. Nuka, S. Pesseat, A. F. Quinn, A. Sangrador-Vegas, M.
811 Scheremetjew, S.-Y. Yong, R. Lopez, S. Hunter, InterProScan 5: genome-scale protein
812 function classification. *Bioinformatics* **30**, 1236–1240 (2014).

813 57. G. Salazar, L. Paoli, A. Alberti, J. Huerta-Cepas, H.-J. Ruscheweyh, M. Cuenca, C. M.
814 Field, L. P. Coelho, C. Cruaud, S. Engelen, A. C. Gregory, K. Labadie, C. Marec, E.
815 Pelletier, M. Royo-Llonch, S. Roux, P. Sánchez, H. Uehara, A. A. Zayed, G. Zeller, M.
816 Carmichael, C. Dimier, J. Ferland, S. Kandels, M. Picheral, S. Pisarev, J. Poulain, Tara
817 Oceans Coordinators, S. G. Acinas, M. Babin, P. Bork, C. Bowler, C. de Vargas, L.
818 Guidi, P. Hingamp, D. Iudicone, L. Karp-Boss, E. Karsenti, H. Ogata, S. Pesant, S.
819 Speich, M. B. Sullivan, P. Wincker, S. Sunagawa, Gene Expression Changes and
820 Community Turnover Differentially Shape the Global Ocean Metatranscriptome. *Cell*
821 **179**, 1068–1083.e21 (2019).

822 58. Z. Gu, R. Eils, M. Schlesner, Complex heatmaps reveal patterns and correlations in
823 multidimensional genomic data. *Bioinformatics* **32**, 2847–2849 (2016).

824 59. L. M. van der Loos, R. Nijland, Biases in bulk: DNA metabarcoding of marine
825 communities and the methodology involved. *Mol. Ecol.* **30**, 3270–3288 (2021).

826 60. S. K. Davy, D. Allemand, V. M. Weis, Cell biology of cnidarian-dinoflagellate symbiosis.
827 *Microbiol. Mol. Biol. Rev.* **76**, 229–261 (2012).

828 61. W. K. Kwong, J. Del Campo, V. Mathur, M. J. A. Vermeij, P. J. Keeling, A widespread

coral-infecting apicomplexan with chlorophyll biosynthesis genes. *Nature* **568**, 103–107 (2019).

62. A. Oren, G. M. Garrity, Valid publication of the names of forty-two phyla of prokaryotes. *Int. J. Syst. Evol. Microbiol.* **71** (2021).

63. A. Cárdenas, J.-B. Raina, C. Pogoreutz, N. Rädecker, J. Bougoure, P. Guagliardo, M. Pernice, C. R. Voolstra, Greater functional diversity and redundancy of coral endolithic microbiomes align with lower coral bleaching susceptibility. *ISME J.* **16**, 2406–2420 (2022).

64. J. R. Guest, J. Low, K. Tun, B. Wilson, C. Ng, D. Raingeard, K. E. Ulstrup, J. T. I. Tanzil, P. A. Todd, T. C. Toh, D. McDougald, L. M. Chou, P. D. Steinberg, Coral community response to bleaching on a highly disturbed reef. *Sci. Rep.* **6**, 20717 (2016).

65. P. Buerger, G. M. Schmidt, M. Wall, C. Held, C. Richter, Temperature tolerance of the coral Porites lutea exposed to simulated large amplitude internal waves (LAIW). *J. Exp. Mar. Bio. Ecol.* **471**, 232–239 (2015).

66. J. Peng, C.-E. Wegner, Q. Bei, P. Liu, W. Liesack, Metatranscriptomics reveals a differential temperature effect on the structural and functional organization of the anaerobic food web in rice field soil. *Microbiome* **6**, 169 (2018).

67. N. Vannier, F. Mesny, F. Getzke, G. Chesneau, L. Dethier, J. Ordon, T. Thiergart, S. Hacquard, Genome-resolved metatranscriptomics reveals conserved root colonization determinants in a synthetic microbiota. *Nat. Commun.* **14**, 8274 (2023).

68. S. R. Law, A. R. Serrano, Y. Daguerre, J. Sundh, A. N. Schneider, Z. R. Stangl, D. Castro, M. Grabherr, T. Näsholm, N. R. Street, V. Hurry, Metatranscriptomics captures dynamic shifts in mycorrhizal coordination in boreal forests. *Proc. Natl. Acad. Sci. U. S. A.* **119**, e2118852119 (2022).

69. S. Campana, A. Riesgo, E. Jongepier, J. Fuss, G. Muyzer, J. M. de Goeij, Meta-transcriptomic comparison of two sponge holobionts feeding on coral- and macroalgal-dissolved organic matter. *BMC Genomics* **23**, 674 (2022).

70. A. Schoenle, M. Hohlfeld, K. Hermanns, F. Mahé, C. de Vargas, F. Nitsche, H. Arndt, High and specific diversity of protists in the deep-sea basins dominated by diplonemids, kinetoplastids, ciliates and foraminiferans. *Commun Biol* **4**, 501 (2021).

71. S. L. Pichard, L. Campbell, J. H. Paul, Diversity of the ribulose bisphosphate carboxylase/oxygenase form I gene (rbcL) in natural phytoplankton communities. *Appl. Environ. Microbiol.* **63**, 3600–3606 (1997).

72. B. K. Swan, M. Martinez-Garcia, C. M. Preston, A. Sczyrba, T. Woyke, D. Lamy, T. Reinthaler, N. J. Poulton, E. D. P. Masland, M. L. Gomez, M. E. Sieracki, E. F. DeLong, G. J. Herndl, R. Stepanauskas, Potential for chemolithoautotrophy among ubiquitous bacteria lineages in the dark ocean. *Science* **333**, 1296–1300 (2011).

73. J. A. Raven, Contributions of anoxygenic and oxygenic phototrophy and chemolithotrophy to carbon and oxygen fluxes in aquatic environments. *Aquat. Microb. Ecol.* **56**, 177–192 (2009).

74. F. Ricci, C. Greening, Chemosynthesis: a neglected foundation of marine ecology and biogeochemistry: (Trends in Microbiology, Published online January 30, 2024). *Trends Microbiol.* **32**, 723 (2024).

75. M. P. Lesser, M. Sabrina Pankey, M. Slattery, K. J. Macartney, D. J. Gochfeld, Microbiome diversity and metabolic capacity determines the trophic ecology of the holobiont in Caribbean sponges. *ISME Commun.* **2**, 112 (2022).

76. M. Kühl, G. Holst, A. W. D. Larkum, P. J. Ralph, IMAGING OF OXYGEN DYNAMICS WITHIN THE ENDOLITHIC ALGAL COMMUNITY OF THE MASSIVE CORAL PORITES LOBATA(1). *J. Phycol.* **44**, 541–550 (2008).

77. R. Samsonoff Wa Maccoll, Biliproteins and phycobilisomes from cyanobacteria and red algae at the extreme habitats. *Arch* **176**, 400–405 (2001).

78. A. de los Ríos, M. Grube, L. G. Sancho, C. Ascaso, Ultrastructural and genetic characteristics of endolithic cyanobacterial biofilms colonizing Antarctic granite rocks: Antarctic endolithic cyanobacterial biofilms. *FEMS Microbiol. Ecol.* **59**, 386–395 (2007).

79. S. H. Magnusson, M. Fine, M. Kühl, Light microclimate of endolithic phototrophs in the scleractinian corals Montipora monasteriata and Porites cylindrica. *Mar. Ecol. Prog. Ser.* **332**, 119–128 (2007).

80. C. Iha, K. E. Dougan, J. A. Varela, V. Avila, C. J. Jackson, K. A. Bogaert, Y. Chen, L. M. Judd, R. Wick, K. E. Holt, M. M. Pasella, F. Ricci, S. I. Repetti, M. Medina, V. R. Marcelino, C. X. Chan, H. Verbruggen, Genomic adaptations to an endolithic lifestyle in the coral-associated alga Ostreobium. *Curr. Biol.* **31**, 1393–1402.e5 (2021).

81. M. Lichtenberg, A. W. D. Larkum, M. Kühl, Photosynthetic Acclimation of Symbiodinium in hospite Depends on Vertical Position in the Tissue of the Scleractinian Coral Montastrea curta. *Front. Microbiol.* **7**, 230 (2016).

82. O. Hoegh-Guldberg, P. J. Mumby, A. J. Hooten, R. S. Steneck, P. Greenfield, E. Gomez, C. D. Harvell, P. F. Sale, A. J. Edwards, K. Caldeira, N. Knowlton, C. M. Eakin, R. Iglesias-Prieto, N. Muthiga, R. H. Bradbury, A. Dubi, M. E. Hatziolos, Coral reefs under rapid climate change and ocean acidification. *Science* **318**, 1737–1742 (2007).

83. N. Rädecker, C. Pogoreutz, H. M. Gegner, A. Cárdenas, F. Roth, J. Bougoure, P. Guagliardo, C. Wild, M. Pernice, J.-B. Raina, A. Meibom, C. R. Voolstra, Heat stress destabilizes symbiotic nutrient cycling in corals. *Proc. Natl. Acad. Sci. U. S. A.* **118** (2021).

84. J. Ji, L. Yang, Z. Fang, Y. Zhang, M. Zhuang, H. Lv, Y. Wang, Plant SWEET Family of Sugar Transporters: Structure, Evolution and Biological Functions. *Biomolecules* **12** (2022).

85. O. Hoegh-Guldberg, Climate change, coral bleaching and the future of the world's coral reefs. *Mar. Freshwater Res.* **50**, 839–866 (1999).

86. A. Roik, M. Reverter, C. Pogoreutz, A roadmap to understanding diversity and function of coral reef-associated fungi. *FEMS Microbiol. Rev.* **46** (2022).

87. A. R. Mohamed, M. A. Ochsenkühn, A. M. Kazlak, A. Moustafa, S. A. Amin, The coral microbiome: towards an understanding of the molecular mechanisms of coral-microbiota interactions. *FEMS Microbiol. Rev.* **47** (2023).

88. N. D. Olson, T. D. Ainsworth, R. D. Gates, M. Takabayashi, Diazotrophic bacteria associated with Hawaiian Montipora corals: Diversity and abundance in correlation with symbiotic dinoflagellates. *J. Exp. Mar. Bio. Ecol.* **371**, 140–146 (2009).

89. K. A. Lema, B. L. Willis, D. G. Bourne, Amplicon pyrosequencing reveals spatial and temporal consistency in diazotroph assemblages of the Acropora millepora microbiome. *Environ. Microbiol.* **16**, 3345–3359 (2014).

90. K. A. Lema, D. G. Bourne, B. L. Willis, Onset and establishment of diazotrophs and other bacterial associates in the early life history stages of the coral Acropora millepora. *Mol. Ecol.* **23**, 4682–4695 (2014).

91. C. Cook, C. D'Elia, Are natural populations of zooxanthellae ever nutrient-limited? *Symbiosis* **4**, 199–211 (1987).

92. J. Li, Q. Yang, J. Dong, M. Sweet, Y. Zhang, C. Liu, Y. Zhang, X. Tang, W. Zhang, S. Zhang, Microbiome Engineering: A Promising Approach to Improve Coral Health. *Proc. Est. Acad. Sci. Eng.* **28**, 105–116 (2023).

93. M. A. Moran, B. P. Durham, Sulfur metabolites in the pelagic ocean. *Nat. Rev. Microbiol.* **17**, 665–678 (2019).

94. T. Higuchi, K. Tanaka, K. Shirai, I. Yuyama, T. Mezaki, N. Takahata, Y. Sano, Sulfur assimilation in corals with aposymbiotic and symbiotic zooxanthellae. *Environ. Microbiol. Rep.* **13**, 98–103 (2021).

95. B. Meyer, J. Kuever, Homology modeling of dissimilatory APS reductases (AprBA) of sulfur-oxidizing and sulfate-reducing prokaryotes. *PLoS One* **3**, e1514 (2008).

96. T. Watanabe, H. Kojima, M. Fukui, Identity of major sulfur-cycle prokaryotes in freshwater lake ecosystems revealed by a comprehensive phylogenetic study of the dissimilatory adenylylsulfate reductase. *Sci. Rep.* **6**, 36262 (2016).

97. J. F. Imhoff, Biology of green sulfur bacteria, *eLS* (2014). https://doi.org/10.1002/9780470015902.a0000458.pub2.

98. C. Ng, M. Z. DeMaere, T. J. Williams, F. M. Lauro, M. Raftery, J. A. E. Gibson, C. Andrews-Pfannkoch, M. Lewis, J. M. Hoffman, T. Thomas, R. Cavicchioli, Metaproteogenomic analysis of a dominant green sulfur bacterium from Ace Lake, Antarctica. *ISME J.* **4**, 1002–1019 (2010).

99. Y.-H. Chen, S.-H. Yang, K. Tandon, C.-Y. Lu, H.-J. Chen, C.-J. Shih, S.-L. Tang, Potential syntrophic relationship between coral-associated Prosthecochloris and its companion sulfate-reducing bacterium unveiled by genomic analysis. *Microb Genom* **7** (2021).

100. I. Kushkevych, J. Cejnar, J. Treml, D. Dordević, P. Kollar, M. Vítězová, Recent Advances in Metabolic Pathways of Sulfate Reduction in Intestinal Bacteria. *Cells* **9** (2020).

101. J. Helgoe, S. K. Davy, V. M. Weis, M. Rodriguez-Lanetty, Triggers, cascades, and endpoints: connecting the dots of coral bleaching mechanisms. *Biol. Rev. Camb. Philos. Soc.* **99**, 715–752 (2024).

102. A. M. Dungan, D. Bulach, H. Lin, M. J. H. van Oppen, L. L. Blackall, Development of a free radical scavenging bacterial consortium to mitigate oxidative stress in cnidarians. *Microb. Biotechnol.* **14**, 2025–2040 (2021).

103. N. Delgadillo-Ordoñez, N. Garcias-Bonet, I. Raimundo, F. C. García, H. Villela, E. O. Osman, E. P. Santoro, J. Curdia, J. G. D. Rosado, P. Cardoso, A. Alsaggaf, A. Barno,

C. P. Antony, C. Bocanegra, M. L. Berumen, C. R. Voolstra, F. Benzoni, S. Carvalho, R. S. Peixoto, Probiotics reshape the coral microbiome in situ without detectable off-target effects in the surrounding environment. *Commun Biol* **7**, 434 (2024).

104. C. R. Voolstra, J.-B. Raina, M. Dörr, A. Cárdenas, C. Pogoreutz, C. B. Silveira, A. R. Mohamed, D. G. Bourne, H. Luo, S. A. Amin, R. S. Peixoto, The coral microbiome in sickness, in health and in a changing world. *Nat. Rev. Microbiol.*, doi: 10.1038/s41579-024-01015-3 (2024).

105. M. J. H. van Oppen, J.-B. Raina, Coral holobiont research needs spatial analyses at the microbial scale. *Environ. Microbiol.* **25**, 179–183 (2023).

106. D. J. Hughes, J.-B. Raina, D. A. Nielsen, D. J. Suggett, M. Kühl, Disentangling compartment functions in sessile marine invertebrates. *Trends Ecol. Evol.* **37**, 740–748 (2022).